Eur. Phys. J. E (2015) **38**: 24
DOI 10.1140/epje/i2015-15024-5

THE EUROPEAN PHYSICAL JOURNAL E

Regular Article

Contribution to the benchmark for ternary mixtures: Measurement of the Soret and thermodiffusion coefficients of tetralin+isobutylbenzene+n-dodecane at a composition of (0.8/0.1/0.1) mass fractions by two-color optical beam deflection*

M. Gebhardt and W. Köhler[a]

Physikalisches Institut, Universität Bayreuth, D-95440 Bayreuth, Germany

Received 15 July 2014 and Received in final form 20 October 2014
Published online: 24 April 2015 –

Abstract. Within the framework of an international benchmark test we have performed measurements of the Soret and thermodiffusion coefficients of the organic ternary mixture (0.8/0.1/0.1 mass fraction) of 1,2,3,4-tetrahydronaphthaline (THN), isobutylbenzene (IBB) and n-dodecane (nC12) at 298.15 K by means of a two-color optical beam deflection technique (OBD). The data evaluation procedure is based on a least squares fitting routine for an approximate analytical solution for the Soret cell problem. The condition number of the contrast factor matrix and standard error propagation are used for an error estimation for the measured Soret and thermodiffusion coefficients. The Soret coefficients obtained are $S'_T(\mathrm{THN}) = (1.20 \pm 0.09) \times 10^{-3}\,\mathrm{K}^{-1}$, $S'_T(\mathrm{IBB}) = (-0.34 \pm 0.14) \times 10^{-3}\,\mathrm{K}^{-1}$, and $S'_T(n\mathrm{C12}) = (-0.86 \pm 0.06) \times 10^{-3}\,\mathrm{K}^{-1}$ and the corresponding thermodiffusion coefficients are $D'_T(\mathrm{THN}) = (0.72 \pm 0.26) \times 10^{-12}\,\mathrm{m}^2(\mathrm{s\,K})^{-1}$, $D'_T(\mathrm{IBB}) = (-0.22 \pm 0.42) \times 10^{-12}\,\mathrm{m}^2(\mathrm{s\,K})^{-1}$, and $D'_T(n\mathrm{C12}) = (-0.50 \pm 0.16) \times 10^{-12}\,\mathrm{m}^2(\mathrm{s\,K})^{-1}$. These results will be used as ground-based reference data for the DCMIX project, where thermodiffusion experiments of ternary mixtures are measured in a microgravity environment aboard the International Space Station (ISS).

1 Introduction

More than a decade ago a successful effort was undertaken to establish reliable benchmark values for the Soret, diffusion, and thermal diffusion coefficients of the three binary mixtures of 1,2,3,4-tetrahydronaphthalene (tetralin, THN), isobutylbenzene (IBB) and n-dodecane (nC12) for a concentration of 50 wt% [1]. The techniques available at this time were transient holographic gratings [2,3], annular and parallelepipedic thermogravitational columns [4], vertical parallelepipedic columns with velocity amplitude determination by laser doppler velocimetry [5], and thermogravitational columns filled with porous media [6]. Additionally, diffusion coefficients were measured by means of the open ended capillary technique [5]. These three binary mixtures became known as the *Fontainebleau benchmark systems*, and new experimental techniques, such as optical digital interferometry (ODI) [7], optical beam deflection (OBD) [8], and a thermogravitational microcolumn [9] have subsequently been validated against these benchmark values. Although the actual experiments can be quite challenging, the experimental concept in case of binary mixtures is rather simple: a temperature gradient leads to a composition change, which is then analyzed. Since there is only one independent concentration variable, the measurement of a single physical parameter, like density or refractive index, is sufficient to obtain all necessary information.

The investigation of ternary liquid mixtures is significantly more complex than the binary case and has gained momentum only during recent years. While binary mixtures are fully characterized by one diffusion and one thermodiffusion coefficient, there are four independent diffusion coefficients and two thermodiffusion coefficients in the ternary case. The diffusion dynamics is characterized by two independent time constants, corresponding to the eigenvalues of the diffusion matrix.

Traditional optical techniques utilize a single laser beam for detection of refractive index changes and can only extract four independent parameters —two amplitudes and two time constants— which is not sufficient for the characterization of a ternary system. In order to extract all six independent coefficients, the missing information must be provided by an additional measurement

* Contribution to the Topical Issue "Thermal non-equilibrium phenomena in multi-component fluids" edited by Fabrizio Croccolo and Henri Bataller.

[a] e-mail: werner.koehler@uni-bayreuth.de

at another wavelength, thereby relying on the different refractive index dispersions of the individual compounds. Such a two-color OBD technique has been proposed by Haugen and Firoozabadi [10] and implemented by Königer *et al.* [11]. A two-color ODI instrument, whose operation is based on similar principles, is available at the International Space Station (ISS) and employed for measurements of ternary mixtures in a microgravity environment within the framework of the DCMIX program [12]. Because of the experimental difficulties encountered with ternary mixtures and because of the success of the Fontainebleau benchmark for the binary mixtures, a number of groups have agreed on a test of their experimental techniques and are aiming to provide benchmark values for a ternary mixture. The selected system is a mixture of tetralin, isobutylbenzene, and *n*-dodecane at a composition of (0.8/0.1/0.1) weight fractions. The choice of this system has been motivated by the ample experience with and data for the corresponding binary mixtures [1, 13] and the choice of these compounds for the first round of the microgravity experiments aboard the ISS (DCMIX1). The choice of the particular composition results from the requirement of an acceptable condition of the contrast factor matrix and because it is one of the five compositions investigated during the DCMIX1 campaign. In this contribution we report in detail on the investigation of this system by means of two-color optical beam deflection as our contribution to the benchmark effort for the characterization of the Soret effect in ternary mixtures.

2 Theory

2.1 The transport coefficients

From an experimental point of view, thermodiffusion in a ternary mixture of density ρ in the absence of convection is fully specified by the flow densities $\mathbf{j}_1$ and $\mathbf{j}_2$ of the two independent components:

$$\mathbf{j}_1 = -\rho \left(D_{11} \nabla c_1 + D_{12} \nabla c_2 + D'_{T,1} \nabla T \right), \tag{1}$$

$$\mathbf{j}_2 = -\rho \left(D_{21} \nabla c_1 + D_{22} \nabla c_2 + D'_{T,2} \nabla T \right). \tag{2}$$

Here, c_1 and c_2 are the corresponding mass fractions and $D'_{T,1}$ and $D'_{T,2}$ the thermodiffusion coefficients. D_{11} and D_{22} are the diagonal and D_{12} and D_{21} are the off-diagonal or cross diffusion coefficients. In a short-hand notation, eqs. (1) and (2) can be written as

$$\underline{\mathbf{j}} = -\rho \left(\underline{\underline{\mathbf{D}}} \, \underline{\nabla c} + \nabla T \, \underline{D'_T} \right), \tag{3}$$

where $\underline{\mathbf{j}} = (\mathbf{j}_1, \mathbf{j}_2)^T$ and $\underline{\nabla c} = (\nabla c_1, \nabla c_2)^T$ are column vectors in the 2d space of the independent concentrations. The vector components themselves are vectors in 3d real space. $\underline{D'_T} = (D'_{T,1}, D'_{T,2})^T$ is a 2d vector with scalar components and $\underline{\underline{\mathbf{D}}}$ is the 2×2 diffusion matrix with scalar entries D_{ij} $(i, j = 1, 2)$.

In the steady state all flows vanish, $\underline{\mathbf{j}} = 0$, and the stationary concentrations gradients are

$$\underline{\nabla c} = -\nabla T \, \underline{S'_T}, \tag{4}$$

where the Soret coefficients have been introduced as

$$\begin{aligned} \begin{pmatrix} S'_{T,1} \\ S'_{T,2} \end{pmatrix} &= \underline{S'_T} = \underline{\underline{\mathbf{D}}}^{-1} \underline{D'_T} \\ &= \frac{1}{D_{11} D_{22} - D_{12} D_{21}} \begin{pmatrix} D_{22} D'_{T,1} - D_{12} D'_{T,2} \\ D_{11} D'_{T,2} - D_{21} D'_{T,1} \end{pmatrix}. \end{aligned} \tag{5}$$

When combined with the equation of continuity for mass conservation, a set of two coupled diffusion equations is obtained that provides a suitable starting point for the description of experiments:

$$\frac{\partial \underline{c}}{\partial t} = \underline{\underline{\mathbf{D}}} (\nabla^2 \underline{c}) + \underline{D'_T} \nabla^2 T. \tag{6}$$

A detailed discussion of the solution of the diffusion equations (6) can be found in the paper of Haugen *et al.* [10]. Alternatively, the two coupled PDEs can directly be integrated on a computer as done by Königer *et al.* [11].

3 Experimental

The two-color OBD-setup (fig. 1) has already been described in a very similar configuration in ref. [11]. Its single-color counterpart for the measurement of binary mixtures had originally been developed in the group of Piazza [14] and was later slightly modified by Königer *et al.* [11].

The main optical components are supported by a sturdy optical rail. The two lasers operate at $\lambda_1 = 405\,\mathrm{nm}$ (Sharp GH04P21A2GE) and $\lambda_2 = 635\,\mathrm{nm}$ (Schäfter und Kirchhoff 51nanoFCM-635) wavelength. This combination of a red wavelength and one near the UV-absorption of aromatic π-electron systems allows for the utilization of the strong refractive index dispersion of these compounds. The two laser beams are combined and coupled into a common single-mode fiber (Schäfter und Kirchhoff, SMC-400-2,6-NA012-3-APC-0-300). The fiber is chosen such that it retains its single-mode property for both wavelength at the expense of an acceptable loss at 635 nm. Both beams are coupled out by a collimator that is mounted on the optical rail by means of an adjustable holder. Because of the optical fiber, all beam pointing instabilities of the lasers are efficiently eliminated.

The main parts of the sample cell are two horizontal copper plates, which can independently be heated and cooled by means of Peltier elements. Clamped between these two copper plates is a glass frame with a geometric path length of $l = 10.0\,\mathrm{mm}$ and a height of $h = 1.43\,\mathrm{mm}$. The laser beams that traverse the diffusion cell are deflected by the refractive index gradients $\partial n_k / \partial z$ (k indicates the wavelength λ_k), which are caused by the change

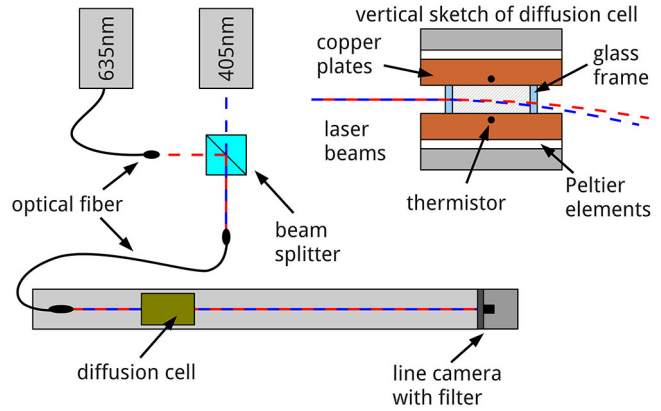

Fig. 1. Two-color optical beam deflection setup with vertical cross section of the Soret (diffusion) cell.

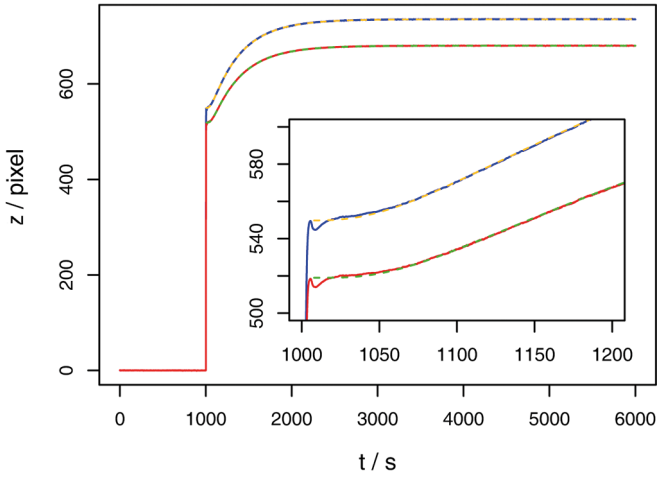

Fig. 2. Measured (solid lines) two-color OBD signals and fit curves (dashed lines) for analytical solutions. Mean temperature $T = 298.15\,\mathrm{K}$. Temperature difference between hot and cold plate 1.0 K, pixel size 8.0 μm.

of temperature, $(\partial n_k/\partial T)_{p,c_j}$, and the change of the concentrations, $(\partial n_k/\partial c_i)_{p,T,c_{j\neq i}}$.

A line camera (EURECA Messtechnik GmbH, USB-Board-TCD1304) at a distance of $l_d = 1.32\,\mathrm{m}$ from the sample cell records the displacements of the laser beams (fig. 2), which is given by

$$\delta z_k = l \left\langle \frac{\partial n_k}{\partial z} \right\rangle \left(\frac{l}{2n_k} + \frac{l_w}{n_{w,k}} + \frac{l_d}{n_{\mathrm{air},k}} \right), \qquad (7)$$

where l_w, $n_{w,k}$ and $n_{\mathrm{air},k}$ are the thickness of the glass window and the refractive indices of the glass and air at the given wavelengths λ_k. Due to the finite width of the laser beams, the refractive index gradient needs to be averaged across the beam profiles as suggested by Kolodner [15]. The refractive index gradient for one particular wavelength can be written as

$$\frac{\partial n_k}{\partial z} = \left(\frac{\partial n_k}{\partial T}\right)_{p,c_i,c_j} \frac{\partial T}{\partial z} + \left(\frac{\partial n_k}{\partial c_i}\right)_{p,T,c_j} \frac{\partial c_i}{\partial z} + \left(\frac{\partial n_k}{\partial c_j}\right)_{p,T,c_i} \frac{\partial c_j}{\partial z}\,. \qquad (8)$$

The temperature of the copper plates is stabilized and switched with a lab-built temperature controller that has already been described in ref. [13]. The temperature jump for the aimed-at temperature is performed ballistically by a previously determined heating or cooling pulse before the PID (proportional-integral-derivative) control sets in. By this technique the heating rate is drastically increased and overshooting of the temperature at the beginning of the deflection signal is eliminated. The temperature is measured by means of calibrated thermistors (Epcos, NTC B57540G0103F00) that are read out by a multimeter (Keithley, Multimeter/Data Acquisition System 2701E).

Refractive indices $n(c_i, c_j, T)$ were measured at 633 nm wavelength with a multi-wavelength Abbe refractometer (Anton Paar Abbemat WR-MW) and at 405 nm with a modified single-wavelength Abbe refractometer (Anton Paar Abbemat WR) at 20 °C. The refractometers were calibrated using calibration liquids provided by Anton Paar with a specified accuracy of 1×10^{-4}. The temperature dependece of the refractive index was measured with an interferometer as described in refs. [3,16].

All measurements were performed with high purity liquids 1,2,3,4-tetrahydronaphthalene (Sigma-Aldrich, 99% anhydrous), isobutylbenzene (Acros Organic, 99.5%) and n-dodecane (Acros Organic, 99%). Mixing by weight fractions was done with a precision balance (Sartorius, BP211D).

4 Results

4.1 Contrast factors

The refractive index of the ternary mixtures was determined on a dense grid in the composition space for 67 sample points at the reference temperature of $T_0 = 20\,^\circ\mathrm{C}$ for the two wavelengths 405 nm and 633 nm. The temperature dependence was measured on a composition grid with 31 sample points between 20 °C and 30 °C. From these data a fit polynomial for a parameterization $n(c_i, c_j, T)$ has been constructed that is quadratic in the temperature $\vartheta = T - T_0$ and cubic in the two concentration variables:

$$n_k(c_i, c_j, T) = \left(1\ c_i\ c_i^2\ c_i^3\right) \left(\underline{\underline{\mathbf{A_0}}} + \underline{\underline{\mathbf{A_1}}}\vartheta + \underline{\underline{\mathbf{A_2}}}\vartheta^2\right) \left(1\ c_j\ c_j^2\ c_j^3\right)^T. \qquad (9)$$

The $\underline{\underline{\mathbf{A_h}}}$ are 4×4 matrices (tables 1–3)

$$\underline{\underline{\mathbf{A_h}}} = \left(a^h_{lm}\right), \quad l, m = 0, 1, 2, 3. \qquad (10)$$

Table 1. Experimentally determined coefficients a^0_{lm} of the matrix $\underline{\underline{\mathbf{A_0}}}$ for the parameterization of the refractive index $n(c_i, c_j, T)$ according to eq. (9).

	(c_3, c_2) *n*C12-IBB		(c_2, c_1) IBB-THN		(c_3, c_1) *n*C12-THN	
	405 nm	633 nm	405 nm	633 nm	405 nm	633 nm
a^0_{00}	1.5716	1.5389	1.4348	1.4207	1.5117	1.4842
a^0_{01}	−0.0653	−0.0595	0.1045	0.0906	0.0548	0.0508
a^0_{02}	0.0058	0.0058	0.0199	0.0173	0.0047	0.0029
a^0_{03}	−0.0004	−0.0010	0.0124	0.0103	0.0004	0.0010
a^0_{10}	−0.1815	−0.1561	0.0635	0.0520	−0.0940	−0.0779
a^0_{11}	0.0362	0.0323	0.0274	0.0250	−0.0196	−0.0168
a^0_{12}	−0.0037	−0.0049	0.0252	0.0196	−0.0025	−0.0020
a^0_{13}	0	0	0	0	0	0
a^0_{20}	0.0570	0.0482	0.0097	0.0087	0.0208	0.0172
a^0_{21}	−0.0119	−0.0114	0.0169	0.0130	0.0058	0.0046
a^0_{22}	0	0	0	0	0	0
a^0_{23}	0	0	0	0	0	0
a^0_{30}	−0.0124	−0.0103	0.0037	0.0028	−0.0037	−0.0028
a^0_{31}	0	0	0	0	0	0
a^0_{32}	0	0	0	0	0	0
a^0_{33}	0	0	0	0	0	0

Table 2. Experimentally determined coefficients a^1_{lm} of the matrix $\underline{\underline{\mathbf{A_1}}}$ for the parameterization of the refractive index $n(c_i, c_j, T)$ according to eq. (9).

	in $10^{-4}\,\mathrm{K}^{-1}$					
	(c_3, c_2) *n*C12-IBB		(c_2, c_1) IBB-THN		(c_3, c_1) *n*C12-THN	
	405 nm	633 nm	405 nm	633 nm	405 nm	633 nm
a^1_{00}	−4.939	−4.672	−4.404	−4.283	−5.156	−4.896
a^1_{01}	−0.193	−0.189	−0.442	−0.312	0.227	0.235
a^1_{02}	−0.029	−0.042	−0.094	−0.077	−0.011	−0.011
a^1_{03}	0	0	0	0	0	0
a^1_{10}	0.806	0.617	−0.639	−0.500	1.030	0.853
a^1_{11}	0	0	0	0	0	0
a^1_{12}	0	0	0	0	0	0
a^1_{13}	0	0	0	0	0	0
a^1_{20}	−0.327	−0.276	−0.119	−0.120	−0.334	−0.289
a^1_{21}	0	0	0	0	0	0
a^1_{22}	0	0	0	0	0	0
a^1_{23}	0	0	0	0	0	0
a^1_{30}	0	0	0	0	0	0
a^1_{31}	0	0	0	0	0	0
a^1_{32}	0	0	0	0	0	0
a^1_{33}	0	0	0	0	0	0

Table 3. Experimentally determined coefficients a^2_{lm} of the matrix $\underline{\underline{\mathbf{A_2}}}$ for the parameterization of the refractive index $n(c_i, c_j, T)$ according to eq. (9).

	in $10^{-7}\,\mathrm{K}^{-2}$					
	(c_3, c_2) nC12-IBB		(c_2, c_1) IBB-THN		(c_3, c_1) nC12-THN	
	405 nm	633 nm	405 nm	633 nm	405 nm	633 nm
a^2_{00}	0.108	0.203	−0.587	−0.544	−0.274	−0.250
a^2_{01}	0.234	−0.437	−0.225	0.324	0.196	0.537
a^2_{02}	−0.775	−0.014	1.017	0.408	0.278	−0.102
a^2_{03}	0	0	0	0	0	0
a^2_{10}	−2.263	−2.237	0.602	−0.230	−1.475	−1.818
a^2_{11}	0	0	0	0	0	0
a^2_{12}	0	0	0	0	0	0
a^2_{13}	0	0	0	0	0	0
a^2_{20}	1.867	1.809	−0.446	0.530	1.458	1.843
a^2_{21}	0	0	0	0	0	0
a^2_{22}	0	0	0	0	0	0
a^2_{23}	0	0	0	0	0	0
a^2_{30}	0	0	0	0	0	0
a^2_{31}	0	0	0	0	0	0
a^2_{32}	0	0	0	0	0	0
a^2_{33}	0	0	0	0	0	0

Table 4. Measured contrast factors and condition numbers for the mixture 0.8/0.1/0.1 of THN-IBB-nC12 at 298.15 K for the three different concentration bases (c_i, c_j).

	nC12-IBB (c_3, c_2)	IBB-THN (c_2, c_1)	nC12-THN (c_3, c_1)	
$(\partial n_{405}/\partial c_i)_{p,T,c_j}$	−0.1667	0.1060	−0.1059	
$(\partial n_{405}/\partial c_j)_{p,T,c_i}$	−0.0609	0.1668	0.0609	
$(\partial n_{633}/\partial c_i)_{p,T,c_j}$	−0.1436	0.0882	−0.0881	
$(\partial n_{633}/\partial c_j)_{p,T,c_i}$	−0.0555	0.1436	0.0555	
$\mathrm{cond}(\underline{\underline{\mathbf{N_c}}})$	109	132	50	
$(\partial n_{405}/\partial T)_{p,c_i,c_j}$	−4.88	−4.88	−4.88	$10^{-4}\,\mathrm{K}^{-1}$
$(\partial n_{633}/\partial T)_{p,c_i,c_j}$	−4.63	−4.63	−4.63	$10^{-4}\,\mathrm{K}^{-1}$

The contrast factors are calculated from the coefficients according to

$$\left(\frac{\partial n_k}{\partial T}\right)_{p,c_i,c_j} = \left(1\ c_i\ c_i^2\ c_i^3\right)\left(\underline{\underline{\mathbf{A_1}}} + 2\underline{\underline{\mathbf{A_2}}}\vartheta\right)\left(1\ c_j\ c_j^2\ c_j^3\right)^T, \quad (11)$$

$$\left(\frac{\partial n_k}{\partial c_i}\right)_{p,T,c_j} = \left(0\ 1\ 2c_i\ 3\,c_i^2\right)\left(\underline{\underline{\mathbf{A_0}}} + \underline{\underline{\mathbf{A_1}}}\vartheta + \underline{\underline{\mathbf{A_2}}}\vartheta^2\right)\left(1\ c_j\ c_j^2\ c_j^3\right)^T, \quad (12)$$

$$\left(\frac{\partial n_k}{\partial c_j}\right)_{p,T,c_i} = \left(1\ c_i\ c_i^2\ c_i^3\right)\left(\underline{\underline{\mathbf{A_0}}} + \underline{\underline{\mathbf{A_1}}}\vartheta + \underline{\underline{\mathbf{A_2}}}\vartheta^2\right)\left(0\ 1\ 2c_j\ 3\,c_j^2\right)^T. \quad (13)$$

The measured refractive index changes $\underline{\delta n} = (\delta n_1, \delta n_2)^T$ are related to the concentration changes $\underline{\delta c} = (\delta c_i, \delta c_j)^T$ by

$$\underline{\delta n} = \underline{\underline{\mathbf{N_c}}}\ \underline{\delta c}. \quad (14)$$

With the short-hand notation $\partial_{c_i} n_k = (\partial n_k/\partial c_i)_{p,T,c_{j\neq i}}$, the contrast factor matrix $\underline{\underline{\mathbf{N_c}}}$ takes the form

$$\underline{\underline{\mathbf{N_c}}} = \begin{pmatrix} \partial_{c_1} n_1 & \partial_{c_2} n_1 \\ \partial_{c_1} n_2 & \partial_{c_2} n_2 \end{pmatrix}. \quad (15)$$

In order to calculate the concentration changes, the contrast factor matrix needs to be inverted.

Since both $\underline{\delta n}$ and $\underline{\underline{\mathbf{N_c}}}$ are experimental quantities that contain errors $\underline{\epsilon_n}$ and $\underline{\underline{\epsilon_{\mathbf{N_c}}}}$, respectively, eq. (14) leads to

Table 5. Measured Soret and thermodiffusion coefficients for the mixture 0.8/0.1/0.1 of THN-IBB-nC12 at 298.15 K for the three possible choices of the independent concentrations. Bold: weighted averages (proposed Soret and thermodiffusion coefficients). Soret coefficients $S'_{T,i}$ in units of $10^{-3}\,\mathrm{K}^{-1}$ and thermodiffusion coefficients $D'_{T,i}$ in units of $10^{-12}\,\mathrm{m}^2/(\mathrm{s\,K})$.

	nC12-IBB (c_3, c_2)	IBB-THN (c_2, c_1)	nC12-THN (c_3, c_1)	**Proposed average**
$S'_{T,1}$ (THN)	1.19 ± 0.08	1.21 ± 0.10	1.21 ± 0.10	$\mathbf{1.20 \pm 0.09}$
$S'_{T,2}$ (IBB)	-0.32 ± 0.13	-0.35 ± 0.15	-0.35 ± 0.16	$\mathbf{-0.34 \pm 0.14}$
$S'_{T,3}$ (nC12)	-0.87 ± 0.05	-0.86 ± 0.06	-0.86 ± 0.06	$\mathbf{-0.86 \pm 0.06}$
$D'_{T,1}$ (THN)	0.72 ± 0.26	0.72 ± 0.26	0.73 ± 0.26	$\mathbf{0.72 \pm 0.26}$
$D'_{T,2}$ (IBB)	-0.21 ± 0.42	-0.22 ± 0.42	-0.23 ± 0.42	$\mathbf{-0.22 \pm 0.42}$
$D'_{T,3}$ (nC12)	-0.51 ± 0.16	-0.50 ± 0.16	-0.50 ± 0.16	$\mathbf{-0.50 \pm 0.16}$

an uncertainty $\underline{\epsilon_c}$ of the concentrations

$$\underline{\delta c} + \underline{\epsilon_c} = \left(\underline{\underline{\mathbf{N_c}}} + \underline{\underline{\epsilon_{\mathbf{N_c}}}}\right)^{-1} \left(\underline{\delta n} + \underline{\epsilon_n}\right). \tag{16}$$

The error amplification encountered by this inversion can be estimated from the condition number of the contrast factor matrix [17,18],

$$\mathrm{cond}(\underline{\underline{\mathbf{N_c}}}) = ||\underline{\underline{\mathbf{N_c}}}||\ ||\underline{\underline{\mathbf{N_c^{-1}}}}||, \tag{17}$$

where $||\ldots||$ denotes the spectral matrix norm (2-norm) [17]. If the condition number is of order cond $\sim 10^{\alpha}$ and the relative error of both the measured refractive index changes and the contrast factors are of order $\sim 10^{-d}$, the relative error of the concentrations will be less than or equal to $10^{\alpha-d+1}$. Although this is a rather pessimistic estimation, it can be used as a guideline to conclude that the condition number should not significantly exceed 10^2. Both the refractive index changes in the Soret cell and the contrast factors need to be measured with a high accuracy in order to provide sufficiently accurate results for the concentration changes and the Soret coefficients.

The contrast factors and the condition numbers are summarized in table 4 for the three possible choices of the independent concentration variables. The transformation of the transport coefficient to another set of independent concentrations can be found in the appendix of ref. [11].

The independent concentrations (c_3, c_1) yield the lowest condition number and, hence, c_2 (IBB) has been chosen as the dependent concentration for the data evaluation. The condition number for this concentration base is shown in fig. 3 for the whole composition range.

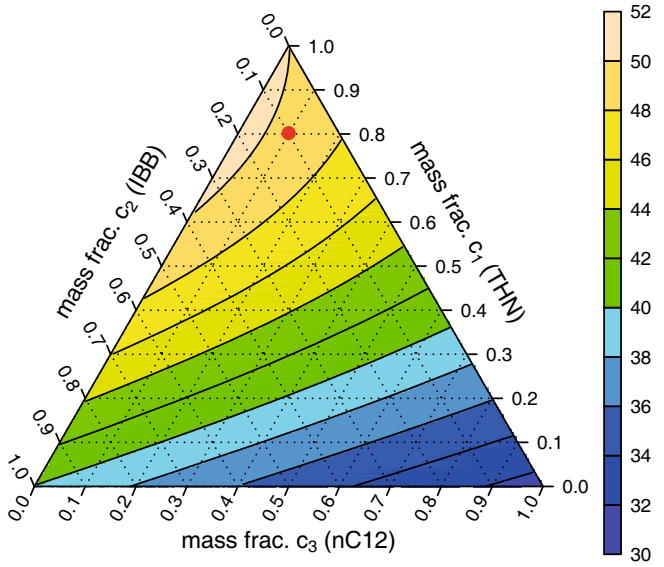

Fig. 3. Condition number of contrast factor matrix for concentration base (c_3, c_1). The red dot indicates the composition for which the Soret coefficient has been determined. $T = 298.15\,\mathrm{K}$.

4.2 Soret coefficients

The stationary concentration amplitudes are obtained from a numerical fit of an analytic solution of the coupled thermodiffusion equations (6) to the measured OBD signals as shown in fig. 2. The Soret coefficients are then determined from the concentration changes according to eq. (4). The Soret coefficient of the dependent component is obtained from $\sum_{i=1}^{3} S'_{T,i} = 0$. The numerical values of the Soret coefficients are summarized in table 5 for all three concentration bases, which yield almost identical results. Since the numbers obtained for the respective coefficients in the three concentration bases slightly differ, we propose as our final results average values for the Soret and thermodiffusion coefficients and their standard deviations. These results are tabulated in the last column in table 5.

The error estimation for the Soret coefficients poses a delicate problem. Experience in our laboratory has shown that the repeatability of the beam deflection amplitudes is of the order of 0.2 percent for amplitudes similar to the one found in the present experiment. After transformation to the concentration changes by multiplication with the inverse of the contrast factor matrix, and, thus, to the Soret coefficients, relative errors of the order of a few percent are obtained, which is almost one order of magnitude less than the worst-case scenario predicted by the simple multiplication with the condition number of the contrast factor matrix. The relative uncertainty of the contrast factors is also of the order of a few tenths of a percent and approximately

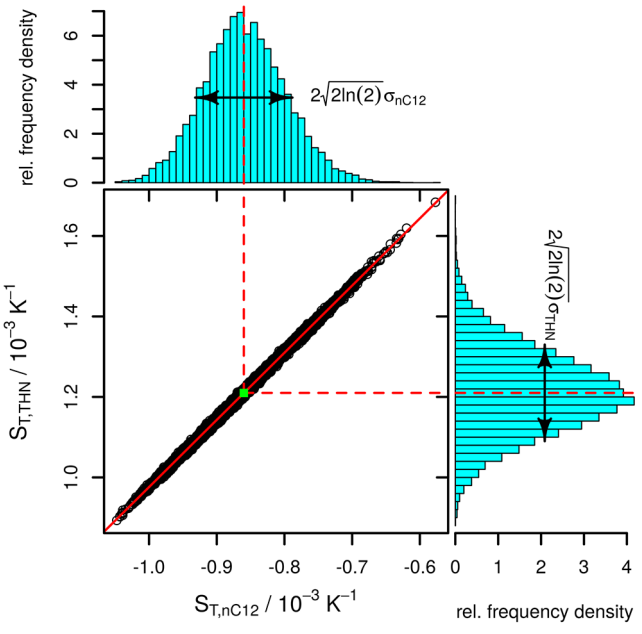

Fig. 4. Distribution of Soret coefficients of nC12 and THN obtained from normally distributed noise of the measured amplitudes and contrast factors. σ_{nC12} and σ_{THN} are the standard deviations as given as errors in table 5. The fitted diagonal line corresponds to eq. (20).

doubles the error to the Soret coefficients. Additional error sources, like a slow baseline drift, low frequency noise and systematic errors, are much harder to identify and their combined effect can only be estimated based on a long experience with the experimental setup. The errors of S'_T in table 5 are obtained on the basis of a statistical simulation of normally distributed noise with a standard deviation of 2×10^{-4} for the contrast factors and 5×10^{-4} for the stationary beam deflection amplitudes (both in absolute numbers) after normalization to the thermal signal. Correlations between the Soret coefficients have not been considered. Interestingly, almost identical standard deviations are obtained by the statistical analysis for the three different concentration bases, although the respective condition numbers differ by more than a factor of two.

The distribution of Soret coefficients is shown in fig. 4 for a simulation of 10^4 pairs of Soret coefficients in case of IBB as the dependent component. The strong correlation is obvious. It allows for the construction of linear relations between pairs of S'_T values that are obtained from the experiments with a much higher accuracy than the individual coefficients (all Soret coefficients in K^{-1})

$$S'_{T,1} = 0.991 \times 10^{-3} - 0.626\, S'_{T,2}, \quad \text{stdev} = 2 \times 10^{-6}, \tag{18}$$

$$S'_{T,2} = -2.641 \times 10^{-3} - 2.668\, S'_{T,3}, \quad \text{stdev} = 4 \times 10^{-6}, \tag{19}$$

$$S'_{T,1} = 2.645 \times 10^{-3} + 1.669\, S'_{T,3}, \quad \text{stdev} = 5 \times 10^{-6}. \tag{20}$$

4.3 Thermodiffusion coefficients

Besides the Soret coefficient the data evaluation by fitting eq. (6) to the measured OBD transients also yields the three thermodiffusion coefficients $D'_{T,i}$. The error estimation is essentially identical to the one discussed in case of the Soret coefficients. The main difference is that D'_T is not encoded in the stationary amplitudes but rather in the change of the OBD signals at short times, which results in a larger relative error. The obtained $D'_{T,i}$ are also listed in table 5.

As in case of the Soret coefficients, correlations with a much smaller error bar than the individual coefficients can also be obtained for the thermodiffusion coefficients (all thermodiffusion coefficients in $m^2(s\,K)^{-1}$)

$$D'_{T,1} = 0.583 \times 10^{-12} - 0.625\, D'_{T,2}, \quad \text{stdev} = 0.5 \times 10^{-14}, \tag{21}$$

$$D'_{T,2} = -1.552 \times 10^{-12} - 2.664\, D'_{T,3}, \quad \text{stdev} = 1.2 \times 10^{-14}, \tag{22}$$

$$D'_{T,1} = 1.552 \times 10^{-12} + 1.664\, D'_{T,3}, \quad \text{stdev} = 1.2 \times 10^{-14}. \tag{23}$$

5 Summary and Conclusions

Two-color optical beam deflection measurements have been carried out in order to determine the Soret and thermodiffusion coefficients of all three components of a ternary mixture of 1,2,3,4-tetrahydronaphthaline (THN), isobutylbenzene (IBB) and n-dodecane (nC12) at 298.15 K with a composition of (0.8/0.1/0.1 mass fraction) as part of a benchmark campaign. The contrast factors have been measured for the entire composition space with a high accuracy. The accuracy requirements for the contrast factors is much more stringent than in case of binary mixtures, since the contrast factor matrix needs to be inverted to determine the Soret coefficients from the measured refractive index changes. In order to profit from the strong dispersion of aromatic compounds near their UV absorption frequencies, one of the lasers has been chosen in the blue spectral range with a wavelength of 405 nm. The second laser is on the red side of the spectrum. Due to this choice of the detection wavelenghts, a reasonable condition number of the contrast factor matrix could be obtained. It should be noted that the detection wavelengths are different from the ones in the SODI apparatus onboard the ISS, where 670 nm and 935 nm are employed. A thorough analysis has shown that it is not possible to extract the diffusion matrix with a comparable accuracy from the OBD data. We are planning to publish a detailed discussion of the associated problems in the near future. For the moment we have limited the evaluation of the OBD measurements to the Soret and thermodiffusion coefficients.

This work was supported by the Deutsche Forschungsgemeinschaft (KO1541/9-2) and by DLR (50WM1130). We thank V. Shevtsova, A. Mialdun, T. Lyubimova, and I. Ryzhkov for valuable hints for the error estimation.

References

1. J.K. Platten *et al.*, Philos. Mag. **83**, 1965 (2003).
2. C. Leppla, S. Wiegand, Philos. Mag. **83**, 1989 (2003).
3. G. Wittko, W. Köhler, Philos. Mag. **83**, 1973 (2003).
4. M.M. Bou-Ali *et al.*, Philos. Mag. **83**, 2011 (2003).
5. J.K. Platten, M.M. Bou-Ali, J.F. Dutrieux, Philos. Mag. **83**, 2001 (2003).
6. P. Costesèque, J.-C. Loubet, Philos. Mag. **83**, 2017 (2003).
7. A. Mialdun, V. Shevtsova, J. Chem. Phys. **134**, 044524 (2011).
8. A. Königer, B. Meier, W. Köhler, Philos. Mag. **89**, 907 (2009).
9. P. Naumann *et al.*, J. Phys. Chem. B **116**, 13889 (2012).
10. K.B. Haugen, A. Firoozabadi, J. Phys. Chem. B **110**, 17678 (2006).
11. A. Königer, H. Wunderlich, W. Köhler, J. Chem. Phys. **132**, 174506 (2010).
12. A. Mialdun *et al.*, Micrograv. Sci. Technol. **25**, 83 (2013).
13. M. Gebhardt *et al.*, J. Chem. Phys. **138**, 114503 (2013).
14. R. Piazza, A. Guarino, Phys. Rev. Lett. **88**, 208302 (2002).
15. P. Kolodner, H. Williams, C. Moe, J. Chem. Phys. **88**, 6512 (1988).
16. A. Becker, W. Köhler, B. Müller, Ber. Bunsenges. Phys. Chem. **99**, 600 (1995).
17. V. Shevtsova, V. Sechenyh, A. Nepomnyashchy, J.C. Legros, Philos. Mag. **91**, 3498 (2011).
18. V. Sechenyh, J.C. Legros, V. Shevtsova, J. Chem. Thermodyn. **62**, 64 (2013).